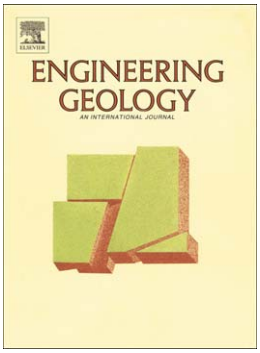

Observations on the Desiccation and Cracking of Clay Layers

R.N. Tollenaar, L.A. van Paassen, C. Jommi

PII: S0013-7952(17)30131-X
DOI: doi:10.1016/j.enggeo.2017.08.022
Reference: ENGEO 4631

To appear in: *Engineering Geology*

Received date: 23 January 2017
Revised date: 6 June 2017
Accepted date: 22 August 2017

Please cite this article as: Tollenaar, R.N., Paassen, L.A. van, Jommi, C., Observations on the Desiccation and Cracking of Clay Layers, *Engineering Geology* (2017), doi:10.1016/j.enggeo.2017.08.022

Observations on the Desiccation and Cracking of Clay Layers

R.N. Tollenaar[a,*], L.A. van Paassen[a,1], C. Jommi[a]

[a]*Department of Geoscience and Engineering, Delft University of Technology, Stevinweg 1, 2628 CN Delft, The Netherlands*
[b]*School of Sustainable Engineering and the Built Environment (SSEBE), Center for Bio-mediated and Bio-inspired Geotechnics (CBBG), Arizona State University, Goldwater Center for Science & Engineering, 650 East Tyler Mall, PO Box 873005, Tempe, AZ 85287-3005, U.S.A.*

Abstract

Waterways and lakes in low-lying delta areas require regular dredging for maintenance. Often these sediments are placed on land, where they are allowed to ripen through a combination of drainage, consolidation and evaporation. When cracks develop during desiccation, the physical response of the soil is affected by changes in the overall strength, stiffness and permeability of the material. To better identify how cracks form and propagate, a series of tests was carried out in a controlled laboratory environment on samples of drying clay slurries under different initial and boundary conditions. The outcomes of this study indicate that the results from laboratory small scale models must be carefully analyzed, as they depend on the area and the thickness of the sample. However, common features from the different tests can be identified, which are mostly related to the intrinsic behavior of the material. For instance, the water content at which cracks initiate depends mostly on the drying rate and not only on the initial water content. Typically for the clayey soil investigated, the cracking water content is well above the shrinkage limit and in some instances even above the liquid limit. Cracks can form anywhere a defect is encountered, but it was observed that they propagate in horizontal directions below the soil surface. On the soil surface they tend to intersect with each other perpendicularly, suggesting

*Corresponding author
Email address: r.n.tollenaar@tudelft.nl (R.N. Tollenaar)

they are dominated by a tensile stress regime. Shear stresses also influence the response, but mainly near to the boundaries of the samples, due to the interface friction.

Keywords:
Clay desiccation, soil drying, fracture propagation, soil cracking

---

1. Introduction

In low-lying delta areas like the Netherlands, the dredging of waterways and lakes is essential for allowing navigation and recreation. Furthermore it helps maintaining the water quality and it allows to efficiently drain the land required for agriculture. One way of dealing with dredged sediments is to store them in upland depots. It has also been suggested that these sediments could be viable as substitute for other materials in civil engineering and agricultural applications. Dredged sediments often contain an important fraction of fines and organic material, all of them with high water contents. Therefore, it requires a significant amount of time for the sediments to ripen through a combination of drainage, consolidation and evaporation.
After enough dewatering has taken place, cracks will start developing, affecting not only the drainage and evaporation, but also producing more deformation. If the dredged material is used in construction, the cracks will affect the physical properties of the material like its strength, stiffness and hydraulic conductivity. While cracks are considered to accelerate evaporation in a ripening soil, they might be detrimental in many civil engineering applications. For instance, they can affect the stability and serviceability of earthworks. Additionally, when the sediments are employed for agricultural purposes, cracks will influence drainage, water infiltration, evaporation, and potentially the soil composition through oxidation and decomposition. Consequently, identifying how cracks occur in the soil is essential for understanding the textcolorredresponse of the material.
Much investigation has already been carried out in geotechnical engineering on desiccation cracks. Kindle (1917) performed the first qualitative experiments looking into the formation of soil cracks. Nevertheless, it was not until Corte and Higashi (1960) that detailed and comprehensive studies into the subject were carried out by analyzing the behavior of clay layers prepared in rectangular containers under different conditions. They looked into the influence of layer thickness, boundary conditions, temperature and humidity

on factors including: fracture intensity, cell size, fracture length, crack patterns and cracking water content. Among their findings are the dependence of the cell size, fracture length and cracking water content on the evaporating soil layer thickness, as well as the effects of the adhesion of the soil to the bottom of the container on the amount of fractures generated. Based on these observations, Corte and Higashi (1960) developed geometrical and mechanical interpretations of the phenomenon. These outcomes have been later corroborated by other researchers, such as Kodikara et al. (2000) who analyzed the data of Corte and Higashi (1960) and Lau (1987), Nahlawi and Kodikara (2006), Lakshmikantha et al. (2006) and Costa et al. (2013). Tang et al. (2008), Tang et al. (2010a) and Costa et al. (2013) were able to show that there was an influence of the desiccation rate in the amount of cracks produced. Rodríguez et al. (2007) observed that the effects of soil thickness on the cracking water content were not noticeable for very thin soil layers. Peron et al. (2009) looked at free and constrained desiccation, and crack patterns. They studied the boundary constraints necessary for cracking, the stages of soil deformation during drying, the relationship between the crack initiation point and the saturation of the material, and crack patterns.

Several theoretical frameworks have been developed to describe the previous experimental observations on fracture initiation and propagation. Some authors have tried to explain the cracking processes using linear elastic fracture mechanics (LEFM), including Morris et al. (1992), Morris et al. (1994), Hallett et al. (1995) and Konrad and Ayad (1997). Hallett and Newson (2005) incorporated the crack-tip opening angle into their LEFM framework, and Prat et al. (2008) took into account the results of fracture toughness and tensile tests in their LEFM model. Abu-Hejleh and Znidarčić (1995) described the cracking process in terms of the consolidation and shrinkage of the desiccating material. Rodríguez et al. (2007) presented a general approach, introducing coupled hydro-mechanical behavior of the soil in unsaturated conditions to simulate the cracking in their laboratory experiments on mine tailings. Shin and Santamarina (2011) utilized an effective stress approach and explained the crack initiation process using the evolution of the air-water interface membrane as the soil dries.

It is generally assumed that soil cracks produced by evaporation start at the surface and propagate downwards. Nonetheless, these assumptions are not corroborated by all the experimental results. Already Corte and Higashi (1960) postulated that propagation occurs towards the surface or the bottom from the center of the layer. Alternatively and based on field observations,

Weinberger (2001) assumed that the most common propagation direction is upwards, starting from the bottom of the layer. Lakshmikantha et al. (2013) noticed during their experiments that cracks started at the bottom of the specimens, propagating vertically upwards and then horizontally.
Both the inception and propagation of desiccation cracks are the result of a combination of material properties, and boundary and internal constraints. These factors are interrelated and it is challenging to clearly distinguish between the respective influences. In this investigation a series of tests were carried out to try to separately evaluate the role of material properties and that of boundary conditions on the initiation and development of cracks in drying clay. This included varying the initial layer thickness, the initial water content, the surface area of the set-up and the container material type. Emphasis is given to the conditions of fracture initiation and propagation, particularly looking at what occurs vertically across the soil layer.

2. Materials and Methods

The investigation was carried out using a commercially available river clay (Ve-Ka, K-10000) from blocks having an original water content of 34 ± 2%. X-ray diffraction analysis showed that the clay is composed (by mass) of 50.2% quartz, 21% vermiculite, 16.2% muscovite, 6.8% anorthite and 5.8% calcite approximately. The physical properties of the clay are shown on Table 1.

Table 1: Physical properties of the clay.

Property		**Value**
Specific Gravity		2.74
Consistency		
	Liquid Limit	57%
	Plasticity Index	33%
	Shrinkage Limit	12%
Soil Classification		CH
Grain Size Analysis		
	Sand	3.1%
	Silt	54.9%
	Clay	42%

All the tests were performed in a climate controlled room with tempera-

ture and relative humidity at 19.0 ± 1 °C and 65 ± 6%, respectively. The air circulation in the room was provided by the air conditioning system, which blew diffused air at several points in the ceiling. To try to achieve homogeneous air flow conditions for the experiments, all containers were placed on the floor of the room, providing a distance of at least 3 m from the air diffusers. Open water evaporation measurements carried out in parallel to the experiments indicated that the imposed conditions corresponded to an average daily evaporation from an open water surface of approximately 2.5 mm/day.

The experiments were mainly carried out using square wooden containers of diverse sizes, with initial clay layer thickness equal to 20, 50 and 100 mm. In order to evaluate the effect of the frictional resistance and adherence to the boundaries, additional tests were carried out using plastic and metal containers.

Haliburton (1978) presented guidelines regarding the storage and desiccation of fine grained dredged materials. He indicated that the end of the free water decant phase (called by him decant point) was around 1.8 times the liquid limit. According to him, after this point the evaporation from the soil is governed by the capillary resupply potential of the soil. This investigation focused on the desiccation of dredged material, therefore the initial water content for the experiments was varied between two and three times the liquid limit (a water content of 114 and 170% respectively). This provided a minimum water decant phase, while also allowing the comparison between different initial conditions. Table 2 shows the full list of performed tests.

Before preparing the clay for the boxes, samples for water content determination were taken from each of the bags containing the clay. Afterwards, clay directly out of the bag was cut into small blocks (each piece averaging approx. 20 mm^3), which were placed in a steel container. Tap water was added until the desired water content was achieved. Subsequently, the steel container was set in a Hobart A200N mixer for 45 minutes at a mixing speed of 200 rpm. The resultant paste was deposited in a plastic container, where it was sealed and left for at least 24 hours to further homogenize. At this point samples of the clay mixture were obtained to test for water content.

The wooden containers were filled with water for at least 48 hours before placing any clay in them. This allowed for the wood to completely saturate before pouring the mud in the boxes to the desired thickness. Even though great care was taken, some air was trapped during the pouring of the mud.

All tests were carried out until the clay was seen to be completely dry at the

Table 2: Summary of the experiments carried out.

Dimensions (m) W x L	Initial Clay Thickness (mm)	Container Material	Water Content (x Liquid Limit)
0.3 x 0.3	20	Wood	3
0.3 x 0.3	50	Wood	2
0.3 x 0.3	50	Wood	3
0.3 x 0.3	100	Wood	2
0.5 x 0.5	20	Wood	3
0.5 x 0.5	50	Wood	3
0.5 x 0.5	100	Wood	2
1 x 1	20	Wood	3
1 x 1	50	Wood	3
1 x 1	100	Wood	2
0.4 x 0.4	40	Metal	2
0.4 x 0.4	40	Metal	3
0.35 x 0.5	50	Plastic	2
0.35 x 0.5	50	Plastic	3

room climatic conditions, which in practice represented a water content of 6 $\pm$ 1%.

The mass change in time was not measured during the tests. Due to the large mass the samples, no weigh scales accurate enough were available to make reliable measurements. Additionally, measuring the overall mass change in time provides only information of the average water content on the entire test, but not at the specific location of the fracture. The water content varies with depth and distance to the boundaries of the crack. Therefore, during the experiments, clay samples were obtained in close proximity to the cracks from some of the tests for water content determination. The soil was extracted using a small auger and it was placed in an oven for 24 hours.

During the tests, pictures of the samples were taken using a Canon 400D camera at 8 megapixels. The pictures were used to measure the approximate cell area, crack length and crack with at the end of the experiments. To correct for perspective the software Perspective Image Correction (Schroeder, 2017) was employed. Digimizer (MedCalc, 2016) was used for the measurement of areas and lengths.

3. Results and Discussion

3.1. General Observations

A summary of the relevant information from the different tests is presented in Table 3.

Figures 1 and 2 present sequences of images showing the evolution of cracks in the clay under different conditions at approximately the beginning, the midpoint and the end of fracturing. Figure 1 compares the evolution of cracks in containers of the same size, but with different initial clay thicknesses. Figure 2 shows fracture progression in containers of different size, but with the same initial clay thickness.

It is clear from Figure 1 that thicker clay layers displayed less cracks, larger intact areas and wider fractures than the thinner ones. This outcome can be partly explained by the different desiccation speeds (e.g. the thinner the layer, the faster it dries) affecting the cracking behavior. Scherer (1990) and Scherer and Smith (1995) pointed out that the drying front tends to be more irregular during fast drying, contributing to the presence of more flaws, which lead to the generation of more fractures.

Figure 2 illustrates the impact that the size of the container can have on the fracture generation. The clay in the 0.3 x 0.3 m and 0.5 x 0.5 m containers produced few and relatively short fractures that did not manage to produce any substantial breakage, nor formation of isolated blocks (i.e. cells). At the end of those tests it was noticed that the dry clay was detached from the bottom of the container, something that did not happen in the 1 x 1 m one. The detachment of the bottom allowed for the relatively free shrinkage of the clay, reducing the magnitude of the tensile forces developed. Because in the 1 x 1 m container the surface of the clay was larger, the overall effect of the friction with the bottom of the container was also higher, allowing for the tensile forces to build up, leading to the eventual fracturing of the clay. The evidence from Figures 1 and 2 highlights some of the relevant factors that need to be taken into consideration during soil cracking experiments when upscaling results from the laboratory to the field and when downscaling field samples to the laboratory. Such factors include the ratio between the area of the setup and the thickness of the soil, the friction provided by the surface of the container and the atmospheric conditions. A variation in cracking was also noted in clay boards with same area and initial thickness, but different initial water content. In the cases with low initial water contents, the final

Table 3: Summary of the test results including initial conditions and the approximate cell areas, length and width of cracks at the end of the tests.

Dim. (m) W x L	Initial Clay Thk. (mm)	Container Material	Initial Water Cont. (%)	Amt. of Cells	Total Cell Area (m^2)	Avg. Cell Area (m^2)	Amt. of Cracks	Avg. Crack Length (mm)	Avg. Crack Width (mm)	Days to First Crack	Total Test Length (Days)
0.3 x 0.3	20	Wood	170	1	0.070	0.070	6	63	2	30	37
0.3 x 0.3	50	Wood	114	2	0.078	0.039	1	299	21	15	59
0.3 x 0.3	50	Wood	170	7	0.060	0.009	8	152	14	29	69
0.3 x 0.3*	100	Wood	114	-	-	-	-	-	-	12	-
0.5 x 0.5	20	Wood	170	1	0.203	0.203	10	122	5	26	37
0.5 x 0.5	50	Wood	170	9	0.181	0.020	11	192	26	37	85
0.5 x 0.5	100	Wood	114	4	0.169	0.042	3	317	36	24	92
1 x 1	20	Wood	170	26	0.841	0.032	62	167	15	40	60
1 x 1	50	Wood	170	22	0.686	0.031	23	255	29	49	102
1 x 1	100	Wood	114	9	0.595	0.066	11	387	39	28	118
0.4 x 0.4	40	Metal	114	1	0.126	0.126	6	144	9	32	49
0.4 x 0.4	40	Metal	170	9	0.119	0.013	11	147	15	42	62
0.35 x 0.5	50	Plastic	114	9	0.118	0.013	10	134	14	33	79
0.35 x 0.5	50	Plastic	170	13	0.114	0.009	13	130	15	35	88

*Sacrificial test.

amount of fractures was lower than in the boards with high initial water contents. Figure 3 and 4 compare the difference in cracking in 0.3 x 0.3 m boards with 50 mm initial thickness at similar stages of drying (i.e. water content).

Additionally there were differences seen in the quantity of cracks that originated in containers of different materials. Most of the fractures in the plastic containers were caused by boundary effects related to the walls. Discarding those fractures, the plastic containers with starting water content of 114% and 170% had a total of one cell with three cracks and two cells with five cracks, respectively. The amount of fractures and cells were lower than in comparable tests using wooden containers, indicating that the plastic provided less friction than the wood. It is known that the base material influences the generation of fractures (Corte and Higashi, 1960; Groisman and Kaplan, 1994; Weinberger, 1999; Peron et al., 2009), given that the tensile forces responsible for cracking originate in part from the resistance of the bottom friction to the shrinkage of the material. The metal container with clay at an initial water content of 114% exhibited fewer cracks with shorter length than similar tests on wood containers. The fractures were not long enough to produce the breakage of the clay into cells. Nevertheless, the other metal container with clay at an initial water content of 170% produced more cracks that were wider, which broke the clay into nine cells. The amount and size of cells were comparable to the 0.5 x 0.5 test on the wooden container with an initial thickness of 50 mm.

Concerning the overall deformations noted through the desiccation of the slurries, at least five distinct deformation stages were observed:

- Stage one: the deformations of the soil were limited to the vertical direction, due mostly to the consolidation of the material;
- Stage two: horizontal deformations, attributable to the shrinkage of the material, complemented the ones observed in phase one. The horizontal deformations were noticeable only after the soil started partially detaching from the walls for the containers;
- Stage three: release of the tensile forces through fracture initiation and propagation;
- Stage four: continued shrinkage with water loss being greater than

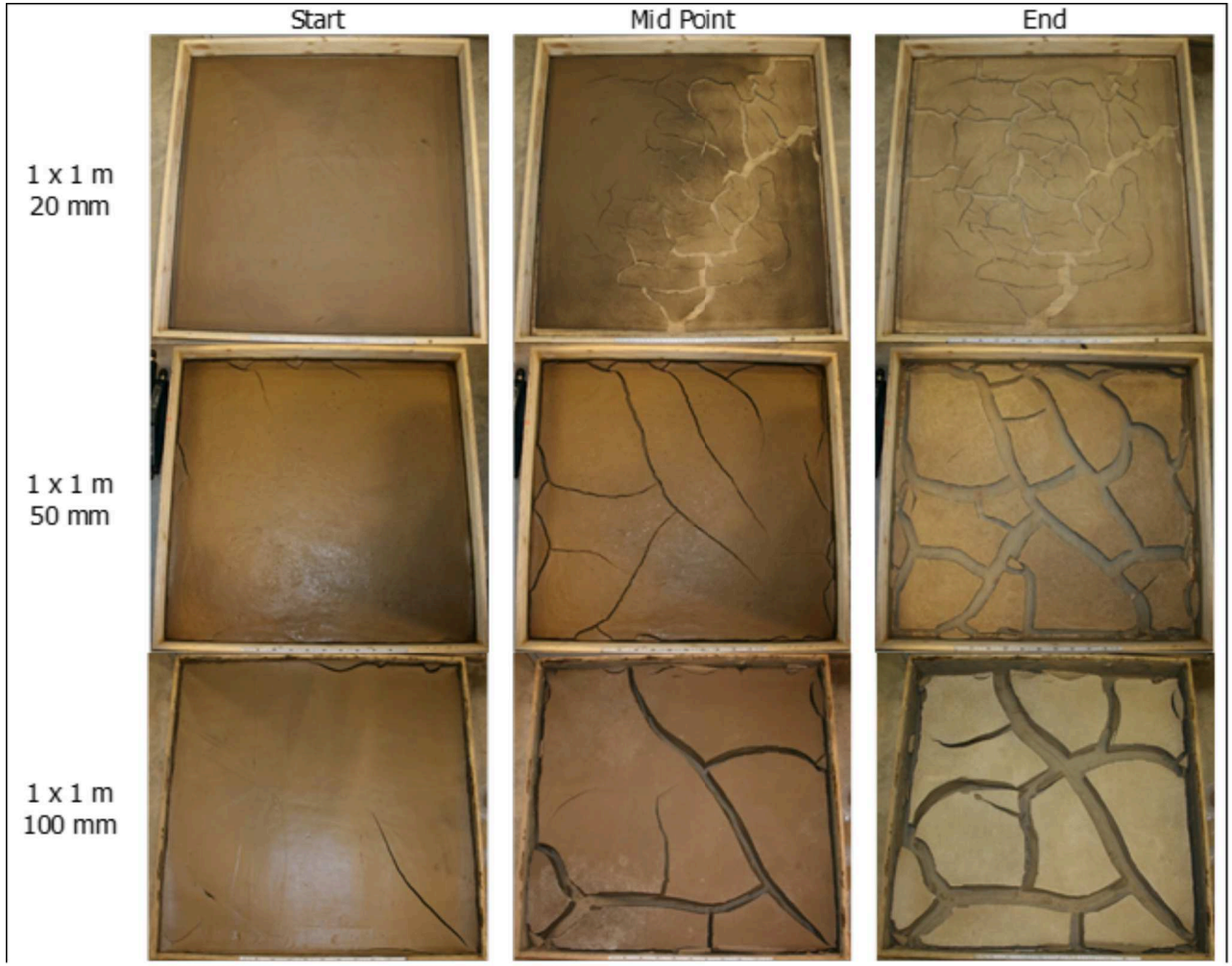

Figure 1: Comparison of the evolution of cracks in containers of the same size, but with different initial clay thicknesses. The general description of each test is located on the left column. The initial water content of the container with an initial thickness of 100 mm was 114%, while in the other two it was 170%.

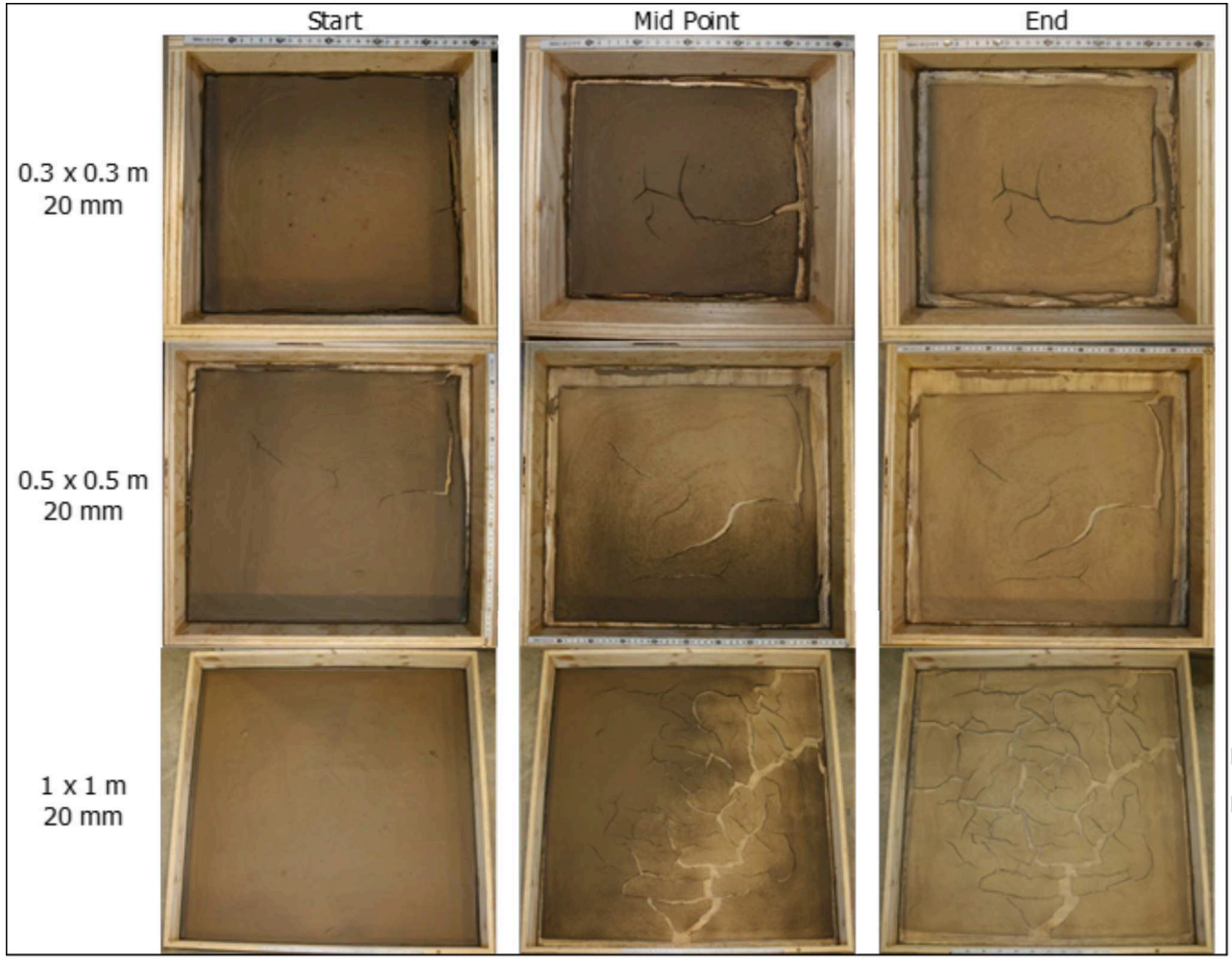

Figure 2: Comparison of the evolution of cracks in containers with the same initial clay thickness, but of different size. The general description of each test is located on the left column.

Figure 3: Cracking in 0.3 x 0.3 m board with 50 mm initial thickness and an initial water content of three times liquid limit approx. (170%).

Figure 4: Cracking in 0.3 x 0.3 m board with 50 mm initial thickness and an initial water content of twice the liquid limit approx. (114%).

the volume decrease (similar to the residual shrinkage described by Bronswijk (1988));

- Stage five: drying without visible shrinkage.

The stages correlate to the phases depicted in the shrinkage curve by Haines (1923) and Bronswijk (1988), and they are similar to the ones described by Abu-Hejleh and Znidarčić (1995). Peron et al. (2009) also defined the deformations during the drying process, but they grouped all in just two steps. In practice, the greatest amount of deformation ensues during the first three stages. The partition between the different stages is difficult to quantify, since they tend to overlap and more than one of the stages can take place at the same time in different sections of the sample.

3.2. Fracture Development and Intersections

In few instances, it was detected that fractures started at locations where a small air bubble trapped in the mud, or an uneven surface was present. The effects on crack initiation of surface defects causing stress concentrations, such as the presence of coarse material, debris, or uneven surfaces, were also observed by Groisman and Kaplan (1994), Zabat et al. (1997), Weinberger (1999) and Tang et al. (2011). The influence of the surface defects was mainly noticeable in the plastic and metal containers. In these two cases, most of the fractures started close to the center of the board, or parallel to the walls of the container as a result of the tensile forces produced by the drying of the soil.

As a general feature in most of the tests, the first fracture started appearing in the clay itself at the interface between the wall of the container and the clay (e.g. Figures 1 and 2). The separation of the clay from the container wall was not considered a fracture, as it was a boundary effect.

The different constraints in the two orthogonal horizontal directions resulted in the cracks generally starting to propagate at angles around 30° from the walls of the container, and in few cases at angles of 45°. The fractures that opened near the corners of the boxes displayed angles of approximately 45°. All the angles other than 90° with respect to the theoretical principal stress direction (i.e. parallel to the edge of the clay) denoted the influence of shear forces at least during the initial stages of the cracking process. The shear forces arose from non-symmetrical boundary conditions imposed by the container, e.g. only partial detachment from the wall, differences in drying,

settlement and adhesion to the bottom, etc. Nonetheless, the fractures that propagated through the clay and eventually reached the edge of the board, did so at an angle of 90°, under tensile crack regime.
The initial cracks generally propagated inwards through the clay. This fractures were the ones that tended to be the widest. After the initial fractures were mostly developed, a second set of cracks appeared, especially in the large boards (1 x 1 m in area). This typically occurred in the boards with an initial thickness of 50 and 100 mm (Figure 1). In the boards with an initial thickness of 20 mm, the first and second set of fractures usually developed in parallel (Figures 2). When the cracks formed cells in the 50 and 100 mm thick boards, they were mostly of regular shapes with four to five sides. In the 20 mm thick experiments that managed to form cells, having very irregular shape and with many sides (Figures 1 and 2).
The tests with initial thicknesses of 50 and 100 mm showed patterns with fractures repeatedly intersecting each other at 90°. Conversely, the boards with 20 mm initial thickness exhibited fracture intersections at both 90° and 120° approximately (Figure 2). The observations showed that the fracture mode was also affected by the thickness of the soil layer. Analogous observations were made by Groisman and Kaplan (1994) during their model desiccation experiments with coffee-water mixtures. Fractures intersecting at 90° and 120° point out to the major influence of tensile and shear forces respectively. Angles of 120° were not observed in the 50 and 100 mm thick layers because the shear forces were relatively small in comparison with the tensile forces produced. Vogel et al. (2005) and Peron et al. (2009) also saw mostly fractures intersecting at 90° and 120°. They both came to similar conclusions relating the 120° junctions to the branching of a crack and the 90° junctions to the coalescence of two fractures, both cases corresponding to the most efficient way of energy dissipation for the particular situation.

3.3. Fracture Initiation and Water Content

The thickness of the material is known to have an effect on the cracking water content. To assess the average water content of the clay at which the cracks started appearing, soil samples of the entire layer thickness were taken from the crack tips, as soon as fracturing was visible. Soil was taken of tests with an initial thicknesses of 20 and 50 mm, with a starting water content of approximately three times liquid limit (170%) and placed in wooden containers. The measurements indicated that in the 20 mm thick layer the first crack became visible after 26 days at an average water content of 48.4%,

compared to 61% for the 50 mm layer after 37 days. A second set of samples was obtained from layers having initial thicknesses of 50 and 100 mm, and a starting water content of approximately twice the liquid limit (114%). The average water content at which the first cracks became visible was approximately 65.6% at 15 days and 83.4% at 12 days, respectively. Nahlawi and Kodikara (2006) indicated that the reduction of cracking water content with the decrease of layer thickness was affected by the increase in average desiccation speed. From the measurements it is also evident that the average cracking water content can be above or below the value at the liquid limit, suggesting that this reference does not provide relevant information on the fracture onset.

To evaluate the development of the water content profile in time in relation to fracture initiation and propagation, samples were taken from a 0.3 x 0.3 m clay board with a starting water content of approximately twice the liquid limit (114%) and an initial thickness of 100 mm. The samples were obtained by removing soil at three different moments in 10 mm intervals for the entire thickness of the layer, beginning when the fracture was first observed and finishing when it crossed the entire board. The material was extracted in close proximity to the location of the fracture tip at the time, and all measurements were made at enough distance from each other, so as to minimize the chances of influence between them. The results are outlined in Table 4. The first crack appeared 12 days after the test was started, and two additional sample sets were obtained at 20 and 30 days.

The effect of the evaporation front was reflected in a lower water content in the upper 10 mm. Below this level the water content remained relatively constant. The maximum water content was located in the bottom quarter to the bottom third of the layer approximately. Due to the small differences in the water content values, the average water content can be considered reasonably representative of the state of the entire layer.

3.4. Observations on Fracture Propagation

During the drying process, linear depressions were observed also on the surface of the clay. As the soil continued drying, these depressions developed into cracks and continued appearing ahead of the opening fracture (Figure 5). It was then evident that the depressions were the surface evidence of a fracture advancing horizontally and under the surface, before emerging at the surface.

Table 4: Water content in percentage (%) with depth, measured at 12 (fracture initiation), 20 and 30 days after the start of the test. he 0.3 x 0.3 m clay board contained soil at an initial water content of approximately twice the liquid limit (114%) and a starting thickness of 100 mm (sacrificial board described in Table 3).

Height from Layer Bottom (mm)	**12 Days**	**20 Days**	**30 Days**
	Water Content (%)		
70-80	76.1	61.4	
60-70	81.9	66.6	52.8
50-40	83.5	68.5	55.7
40-50	84	69.9	59
30-40	85.7	71.3	59.6
20-30	84.3	72.5	58.7
10-20	86.4	70.7	60
0-10	84.9	67.6*	59
Average	83.4	68.6	57.8

*sample not from a full 10 mm interval

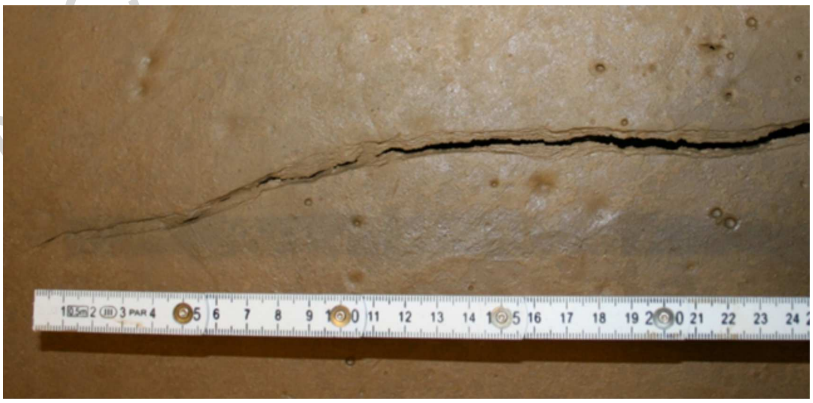

Figure 5: Surface depression on the clay surface ahead of a crack.

The depressions noticed ahead of the cracks were not isolated occurrences during this investigation. They appeared in all the boxes, regardless of their dimensions, bottom material, initial soil thickness and water content. As it is exemplified in Figure 6, they took place in almost every single crack propagating through the soil. However, they were less visible in the 20 mm thick experiments and in the metal container test with an initial water content of twice the liquid limit. During the last stage of drying, the surface depressions stopped appearing ahead of the fractures, possibly due to an increase of stiffness in the upper section of the clay.

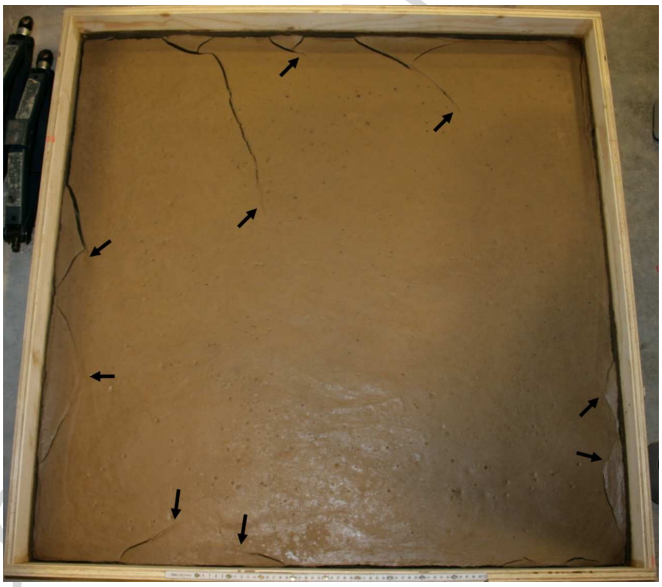

Figure 6: Depressions on the clay indicated with black arrows for a 1 m^2 container with a 50 mm (initial thickness) soil layer and an initial water content of 170%.

Drainage through the bottom of the trays was also not a cause for them, since there was no drainage possible from the plastic and metal containers. Moreover, tests were done with the wooden containers submerged in water, in order to evaluate the permeability of the wood. No perceptible water flow through the wood was seen.
These depressions can also be noticed in the work of Müller and Dahm (2000), Tang et al. (2010b) (Figure 7) and Lakshmikantha et al. (2013). However only Müller and Dahm (2000) and Lakshmikantha et al. (2013) described them, with Müller and Dahm (2000) suggesting that they might be the expression

of the fracture propagating under the surface.

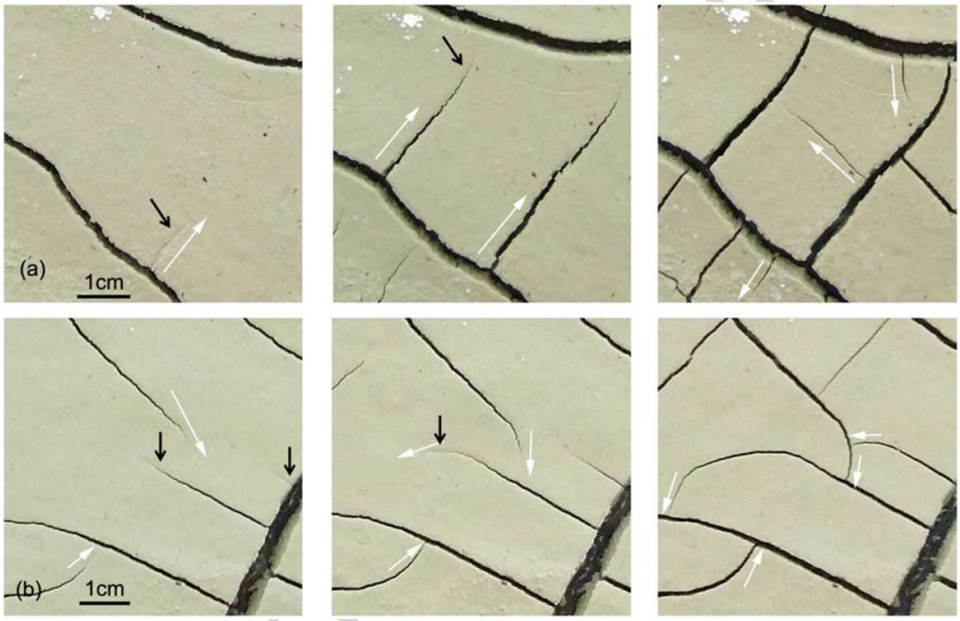

Figure 7: Black arrows pointing to the depressions ahead of the fractures in other experiments (modified from Tang et al. (2010b)).

After the clay fully dried, the walls of the sections or cells formed by the fractures were inspected. Unlike Nahlawi and Kodikara (2002), Kodikara et al. (2004), Peron et al. (2009) and Zielinski et al. (2014), only slight curling of the clay cells in the experiments with 20 mm initial thickness was noticed. In that case, the curling can be attributed to the differential drying between the top and bottom of the sample, as explained by Scherer (1990) and Zielinski et al. (2014). A curvature of the clay surface close to the walls of the containers was detected in most of the tests, but this was a result of boundary effects (differential settlement) and not curling.
Evidence of plumose structures was observed in the cracks from all the containers, no matter what size, tray material, thickness of soil, or initial water content in the tests (Figures 8, 9 and 10).

Plumose fractures were first described by Woodworth (1895, 1896), who observed them in closely spaced parallel joints in argillites. Plumose fractures have also been noted before in lab experiments, such as the ones carried out on soil by Corte and Higashi (1960), cellulose acetate by Kies et al. (1950), by

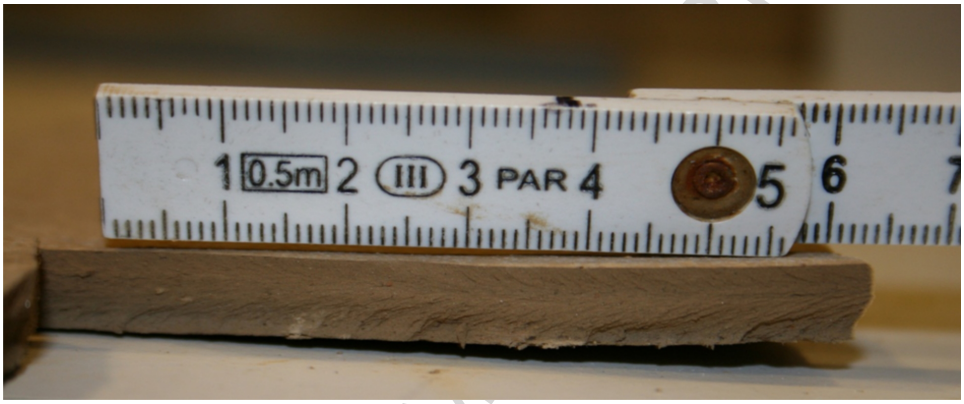

Figure 8: Plumose structures in fractures from container with a 20 mm initial clay thickness.

Figure 9: Plumose structures in fractures from container with a 50 mm initial clay thickness.

Figure 10: Plumose structures in fractures from container with a 100 mm initial clay thickness.

Müller and Dahm (2000) on starch-water mixtures and by Kitsunezaki (2009) on calcium carbonate. Furthermore, they have been seen in clays dried in the field (Weinberger, 1999, 2001; Knight, 2005). These provide information about the direction and mode of failure, with the hackles indicating the overall and local propagation directions of the fracture. The morphology of the plumose structure also shows how the crack front line progresses as the fracture advances (Figure 11).

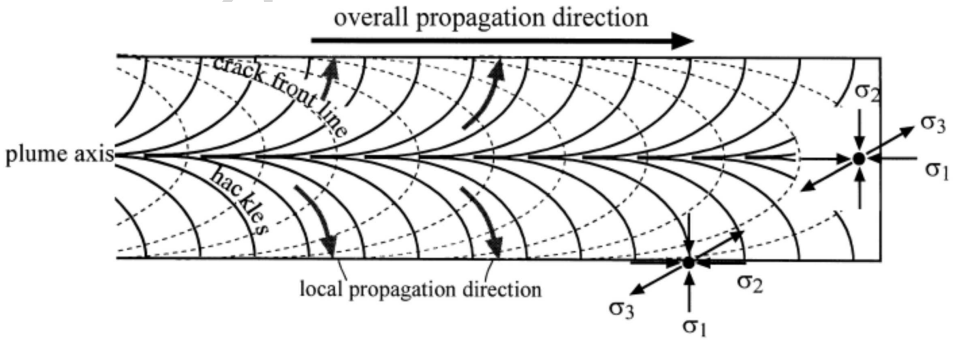

Figure 11: Schematic illustration of a symmetric plumose fracture (Weinberger, 1999).

The experiments with initial thickness of 20 mm displayed quasi-symmetric plumose structures. However, in the tests where thicker layers were used (50 and 100 mm initial thickness), the structures started becoming asymmetric. The location of the plume axis and the crack front line, in addition to the surface depressions observed in front of the cracks, gave a strong indication that the overall propagation of the fractures happened under the surface.

This differs from the common understanding of crack propagation, which is as starting from the surface of the drying soil and advancing vertically downwards. Nonetheless, the local propagation direction might still evolve from sub-horizontal to vertical, as the hackles begin to migrate upwards and downward with fracture propagation.

Corte and Higashi (1960) referred to the plumose fracture description made by Kies et al. (1950). They hypothesized that the cracks started at the center of the soil layer and propagated either to the surface or to the bottom. This is certainly the case at a local scale, but the overall propagation direction and the crack front line do not necessarily follow the same path. Müller and Dahm (2000) recognized that the majority of the fractures in their starch experiments started at the surface, but there were instances where they began at the bottom or at some mid-layer location. Based on his field observations, Weinberger (2001) assumed that most cracks start at or close to the bottom of the layer, propagate upwards and then horizontally. Something similar was noticed by Lakshmikantha et al. (2013) during their experiments. Peron et al. (2009) could not determine, if fractures started at the top or the bottom of the layer in their clay slab tests. However, Kitsunezaki (2009), Shin and Santamarina (2011) and (Tang et al., 2010b, 2011) mentioned that cracks always start at the surface of the layer.

What was observed during the experiments in this study is that the fractures might start anywhere along the depth of the layer (Figure 12). The exact location of initiation would be very difficult to establish, since it would require detailed knowledge of all the forces at every single point in the clay. Yet the general area where the fracture might originate can be deduced, and it is consistent with locations of local stress concentration (e.g. the edge of the clay board, or a surface disturbance). And unlike it was proposed by Corte and Higashi (1960), it was evident (in the case of these experiments) that the crack front line advanced under the surface.

Based on the observations related to the surface depressions, plumose fractures and water content with depth, it can be established that the fracture propagation in the tests did not occur in the areas of the layer with the lower water contents. The depth of propagation approximately followed the zone at which local the water content was similar to the average value of the entire sample. As it was noted, layers under different starting conditions displayed different cracking water contents. Therefore, water content is not the unique dominant factor in fracture propagation, with the rate of water content change also governing soil behavior.

Figure 12: Example of a fracture starting at the bottom left corner of the layer and advancing under the surface towards the right.

4. Conclusions

A series of tests was carried out in a controlled environment on model samples to study the crack formation in desiccating clay under different initial and boundary conditions, including initial water content, layer thickness, set-up size and material. The following conclusions were drawn based on the observations:

- For the same initial and atmospheric conditions, the thickness of the soil layer significantly influenced the water content at which cracking began. The thicker the layer, the higher the water content at which the crack started. The amount and aperture of the fractures generated were affected by the layer thickness, as well. Thinner layers exhibited more fractures than the thick ones.

- The base material affected the amount of fractures produced. The lower the friction of the base material, the lower the amount of cracks generated.

- Factors such as the ratio between the area of the setup and the thickness of the soil, the friction provided by the surface of the container, initial water content and the atmospheric conditions need to be taken into consideration during soil cracking experiments when upscaling results

from the laboratory to the field and when downscaling field samples to the laboratory.

- From the measurements it was evident that the average cracking water content was well above the plastic limit and could be above or below the value of the liquid limit, suggesting that this reference did not provide relevant information on the fracture onset.

- As a result of evaporation, the water content decreased continuously in time, but the differences in the water content measured with depth during the tests were relatively small (except for the top and bottom few millimeters where the water content was lower than average). Consequently, the average water content seemed to reasonably represent the water content of the entire layer.

- Based on the observations related to the surface depressions, plumose fractures and water content with depth, it can be established that the fracture propagation in the tests happened under the surface. The propagation did not occur in the areas of the layer with the lowest water contents.

- Water content was not the unique dominant factor in fracture initiation and propagation, with the desiccation rate also governing soil behavior.

- The angles between fracture intersections were affected by the thickness of the soil layer. Thin layers presented fractures intersecting at 90º and 120º, highlighting the influence of tensile and shear forces respectively on the response of the clay layer.The angles of the initial fractures that were other than 90º with respect to the theoretical principal stress directions, denoted the influence of shear forces arising from non-symmetrical boundary conditions. As the layer thickness increased, only fractures intersecting at 90º were observed, suggesting that normal tensile stresses govern the material behavior.

5. Acknowledgements

This work had the financial support of the Dutch Technology Foundation STW, which is part of the Netherlands Organization for Scientific Research (NWO). It was also partly funded by the Ministry of Economic Affairs, via

the perspective program BioGeoCivil (grant 11344), and through the CEA-MaS (Civil Engineering Applications for Marine Sediments) project, which was supported by the European Regional Development Funding Through INTERREG IV B. Mr. A. Mulder is acknowledged for his help in building the experimental set up.

References

Abu-Hejleh, A., Znidarčić, D., 1995. Desiccation theory for soft cohesive soils. Journal of Geotechnical Engineering 121 (6), 493–502.

Bronswijk, J. J. B., 1988. Modeling of water balance, cracking and subsidence of clay soils. Journal of Hydrology 97 (3-4), 199–212, doi: 10.1016/0022-1694(88)90115-1.

Corte, A., Higashi, A., 1960. Experimental research on desiccation cracks in soil, Research Report 66. Tech. rep., Wilmette, Illinois: US Army Snow Ice and Permafrost Research Establishment.

Costa, S., Kodikara, J. K., Shannon, B., 2013. Salient factors controlling desiccation cracking of clay in laboratory experiments. Gotechnique 63 (1), 18–29.

Groisman, A., Kaplan, E., 1994. An experimental study of cracking induced by desiccation. EPL (Europhysics Letters) 25 (6), 415–420.

Haines, W. B., 1923. The volume changes associated with variations of water content in soil. J. Agric. Sci 13, 296–310.

Haliburton, T. A., 1978. Guidelines for dewatering/densifying confined dredged material, (No. WES-TR-DS-78-11). Tech. rep., DTIC Document, Army Engineer Waterways Experiment Station, Vicksburg, Mississippi.

Hallett, P. D., Dexter, A. R., Seville, J. P. K., 1995. The application of fracture mechanics to crack propagation in dry soil. European Journal of Soil Science 46 (4), 591–599.

Hallett, P. D., Newson, T. A., 2005. Describing soil crack formation using elasticplastic fracture mechanics. European Journal of Soil Science 56 (1), 31–38.

Kies, J. A., Sullivan, A. M., Irwin, G. R., 1950. Interpretation of fracture markings. Journal of Applied Physics 21 (7), 716–720.

Kindle, E. M., 1917. Some factors affecting the development of mud-cracks. The Journal of Geology 25 (2), 135–144.

Kitsunezaki, S., 2009. Crack propagation speed in the drying process of paste. Journal of the Physical Society of Japan 78 (6), 064801.

Knight, J., 2005. Processes of soft-sediment clast formation in the intertidal zone. Sedimentary Geology 181 (34), 207–214.

Kodikara, J. K., Barbour, S. L., Fredlund, D. G., 2000. Desiccation cracking of soil layers. In: Proceedings of the Asian Conference on Unsaturated Soils, UNSAT-Asia 2000, Singapore. Balkema, pp. 693–698.

Kodikara, J. K., Nahlawi, H., Bouazza, A., 2004. Modelling of curling in desiccating clay. Canadian Geotechnical Journal 41 (3), 560–566.

Konrad, J. M., Ayad, R., 1997. A idealized framework for the analysis of cohesive soils undergoing desiccation. Canadian Geotechnical Journal 34 (4), 477–488.

Lakshmikantha, M. R., Prat, P. C., Ledesma, A., 2006. An experimental study of cracking mechanisms in drying soils. In: Proceedings of the 5th international conference on environmental geotechnics. Thomas Telford, London. pp. 533–540.

Lakshmikantha, M. R., Reig, R., Prat, P. C., Ledesma, A., 2013. Origin and mechanism of cracks seen at the bottom of a desiccating soil specimen. In: Geo-Congress 2013 Stability and Performance of Slopes and Embankments III. ASCE, pp. 790–799.

Lau, J. T. K., 1987. Desiccation cracking of clay soils. Master's thesis, Department of Civil Engineering, University of Saskatchewan, Saskatoon, Canada.

MedCalc, 2016. Digimizer, version 4.6.1. MedCalc Software bvba, Acacialaan 22, 8400 Ostend, Belgium.

Morris, P. H., Graham, J., Williams, D. J., 1992. Cracking in drying soils. Canadian Geotechnical Journal 29 (2), 263–277.

Morris, P. H., Graham, J., Williams, D. J., 1994. Crack depths in drying clays using fracture mechanics. In: Fracture mechanics applied to geotechnical engineering. ASCE, pp. 40–53.

Müller, G., Dahm, T., 2000. Fracture morphology of tensile cracks and rupture velocity. Journal of Geophysical Research: Solid Earth 105 (B1), 723–738.

Nahlawi, H., Kodikara, J. K., 2002. Experimental observations on curling of desiccating clay. In: Juca, J. F. T., De Campos, T. M. P., Marinho, F. A. M. (Eds.), Proc. 3rd International Conference on Unsaturated Soils, UNSAT 2002, Recife, Brazil. A. A. Balkema, Rotterdam, The Netherlands, pp. 553–556.

Nahlawi, H., Kodikara, J. K., 2006. Laboratory experiments on desiccation cracking of thin soil layers. Geotechnical and Geological Engineering 24 (6), 1641–1664.

Peron, H., Hueckel, T., Laloui, L., Hu, L. B., 2009. Fundamentals of desiccation cracking of fine-grained soils: experimental characterisation and mechanisms identification. Canadian Geotechnical Journal 46 (10), 1177–1201.

Prat, P. C., Ledesma, A., Lakshmikantha, M. R., Levatti, H., Tapia, J., 2008. Fracture mechanics for crack propagation in drying soils. In: Proceedings of the 12th International Conference of the International Association for Computer Methods and Advances in Geomechanics, IACMAG. Vol. 12. pp. 1060–1067.

Rodríguez, R., Sánchez, M., Ledesma, A., Lloret, A., 2007. Experimental and numerical analysis of desiccation of a mining waste. Canadian Geotechnical Journal 44 (6), 644–658.

Scherer, G. W., 1990. Theory of drying. Journal of the American Ceramic Society 73 (1), 3–14.

Scherer, G. W., Smith, D. M., 1995. Cavitation during drying of a gel. Journal of Non-Crystalline Solids 189 (3), 197–211.

Schroeder, W., 2017. Perspective Image Correction, version 2.0.0.3. Wolfgang.Schroeder2@gmx.de.

Shin, H., Santamarina, J. C., 2011. Desiccation cracks in saturated fine-grained soils: particle-level phenomena and effective-stress analysis. Géotechnique 61 (11), 961–972.

Tang, C. S., Cui, Y. J., Tang, A. M., Shi, B., 2010a. Experiment evidence on the temperature dependence of desiccation cracking behavior of clayey soils. Engineering Geology 114 (34), 261–266.

Tang, C. S., Shi, B., Liu, C., Gao, L., Inyang, H. I., 2010b. Experimental investigation of the desiccation cracking behavior of soil layers during drying. Journal of Materials in Civil Engineering 23 (6), 873–878.

Tang, C. S., Shi, B., Liu, C., Suo, W. B., Gao, L., 2011. Experimental characterization of shrinkage and desiccation cracking in thin clay layer. Applied Clay Science 52 (12), 69–77.

Tang, C. S., Shi, B., Liu, C., Zhao, L., Wang, B., 2008. Influencing factors of geometrical structure of surface shrinkage cracks in clayey soils. Engineering Geology 101 (34), 204–217.

Vogel, H. J., Hoffmann, H., Roth, K., 2005. Studies of crack dynamics in clay soil: I. Experimental methods, results, and morphological quantification. Geoderma 125 (3), 203–211.

Weinberger, R., 1999. Initiation and growth of cracks during desiccation of stratified muddy sediments. Journal of Structural Geology 21 (4), 379–386.

Weinberger, R., 2001. Evolution of polygonal patterns in stratified mud during desiccation: The role of flaw distribution and layer boundaries. Bulletin of the Geological Society of America 113 (1), 20–31.

Woodworth, J. B., 1895. Some features of joints. Science 2 (52), 903–904.

Woodworth, J. B., 1896. On the fracture system of joints: With remarks on certain fractures. Boston Society of Natural History Proceedings 27, 163–184.

Zabat, M., Vayer-Besançon, M., Harba, R., Bonnamy, S., Van Damme, H., 1997. Surface topography and mechanical properties of smectite films. In: Trends in Colloid and Interface Science XI. Springer, pp. 96–102.

Zielinski, M., Sánchez, M., Romero, E., Atique, A., 2014. Precise observation of soil surface curling. Geoderma 226-227, 85–93.

Highlights

- Results of desiccation tests are affected by the area and thickness of the samples.
- Angles between fracture intersections are affected by the clay layer thickness.
- Propagation of the fractures is systematically observed below the soil surface.
- The rate of drying governs the soil behavior as well as the initial water content.
- The liquid limit does not provide useful information on the average cracking water content.